

## Formation of Internal Structure in the Rolling of a bcc (110)[001] Single Crystal

A. A. Redikul'tsev<sup>a, \*</sup>, A. G. Uritskii<sup>b</sup>, M. P. Puzanov<sup>a</sup>, and A. S. Belyaevskikh<sup>a</sup>

<sup>a</sup>*Yeltsin Ural Federal University, Yekaterinburg, Russia*

<sup>b</sup>*Institute of Engineering Science, Ural Branch, Russian Academy of Sciences, Yekaterinburg, Russia*

\**e-mail: redikultsev@mail.ru*

Received December 27, 2015

**Abstract**—The stages of structure formation during cold rolling are investigated in bcc (110)[001] single crystals of Fe–3% Si alloy, within the deformation zone. To obtain a visible deformation zone, the laboratory mill is abruptly stopped at the instant of sample rolling. To reduce the frictional coefficient, lubricant is used for some of the samples. The deformational structure is studied by metallography and orientational electron microscopy (EBSD). Deform-3D software is used to analyze the relation between the experimental data and the calculated stress state in rolling, for various values of the frictional coefficient. Depending on the frictional coefficient, the stress state may significantly affect the mesostructure formation and the texture development. In a single crystal rolled with elevated friction, when the deformation is relatively small, deformation bands are formed. Orientational analysis of the contact point of deformation bands reveals alternating microbands, each with slight different orientation, which are separated by small-angle boundaries. In the rolling of a (110)[001] single crystal with lubrication (reduced friction), twinning is observed even with slight deformation. The twinning is evidently due to the reduced contribution of surface energy to the total energy of twin nucleation. Throughout the whole deformation process, either the twins of both systems retain the strict  $\Sigma 3$  crystallographic relation with the matrix or else, on account of the local lattice reorientation,  $\Sigma 3$  disorientations are converted to similar special  $\Sigma 17b$  and  $\Sigma 43c$  disorientations. On the basis of experimental data, a dislocation model is proposed for the formation of deformational mesostructures in the cold rolling of a (110)[001] single crystal. This model includes the formation of microbands in the initial stage of deformation-band generation; the formation of transition bands parallel to the rolling plane with the dynamic retention of the initial orientation; and the formation of transition bands inclined to the rolling plane with a habitus parallel to the {112} matrix plane. These inclined planes are equivalent to shear bands whose habitus is inclined at  $\sim 17^\circ$  to the rolling plane.

**Keywords:** rolling, deformation zone, single crystal, deformation bands, transition bands, twinning, special boundaries

**DOI:** 10.3103/S0967091217030111

In rolling mills, the cold deformation of metals and alloys occurs at high speed over brief periods, within a relatively small volume (the deformation zone). Even with small deformation, significant change in structure and texture of the material may be observed, as a result of various processes, such as the systematic triggering of slip systems, twinning, and the localization of deformation in band structures [1–10]. Since attention is usually confined to the final result of rolling, it would be of interest to trace the dynamics of this multistage process.

In the present work, we investigate the stages in mesostructure formation during cold rolling, within the deformation zone. As an example, we study bcc (110)[001] single crystals of Fe–3% Si alloy. This alloy is a good model for the study of deformation processes, in that its single crystals support practically all

known modes of plastic deformation: slipping, twinning, and various localized deformation bands [8–12]. In addition, the alloy is used in industry as an anisotropic electrical steel. In other words, research on its deformation may also be of practical interest [13–16].

### EXPERIMENTAL MATERIALS AND METHODS

We use  $0.5 \times 280 \times 30$  mm plates of the commercial anisotropic electrical steel after removing the electrically insulating coating. The plates consist of large grains (30–50 mm in the rolling plane) and are characterized by perfect (110)[001] texture.

For cold rolling, we use a reversible laboratory four-high rolling mill, with working rollers of diameter 75 mm and width 250 mm; the maximum load is 20 t. The plates are rolled in a single pass, with  $\sim 55\%$  defor-

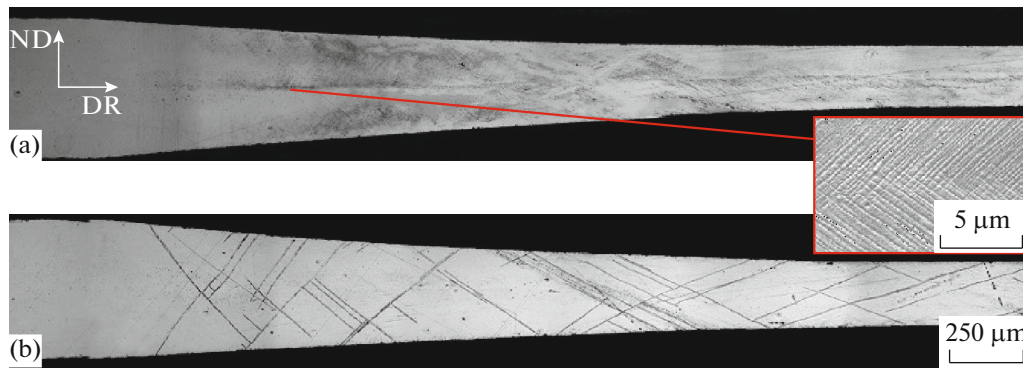


**Fig. 1.** Microstructure of the deformation zone of rolled Fe–3% Si single crystals with initial orientations close to (110)[001]: (a) rolling with elevated friction (without lubrication); (b) rolling with lubrication. Inset: microrelief at surface of section ( $\epsilon \sim 18\%$ ; chemical polishing).

mation, in a direction close to  $\langle 001 \rangle$ . Some of the samples are rolled using lubricant. Others are thoroughly degreased before rolling, and lubricant is removed from the surface of the working rollers. The laboratory mill is abruptly stopped at the instant of sample rolling, so as to obtain a visible deformation zone. Samples are cut from plates where the deformation zone is in the center of a large grain with perfect (110)[001] orientation and subjected to metallographic analysis and orientational analysis on a Carl Zeiss Auriga CrossBeam electron microscope with an Oxford Instruments HKL Nordlys F (EBSD) attachment. The scanning increment is 0.5–1.0  $\mu\text{m}$ ; the error in determining the lattice orientation is no more than  $\pm 1^\circ$  (about  $\sim \pm 0.6^\circ$  on average). Small-angle boundaries between local volumes are plotted on orientation charts when the disorientation is 2–10°; with disorientation of 10° or more, large-angle boundaries are plotted.

The stress state in cold rolling is calculated by the finite-element method, on the basis of Deform-3D software. Coulomb friction is specified at steel–roller contact. The frictional coefficient is assumed to be  $\mu = 0.22$  in the absence of lubricant and  $\mu = 0.11$  with lubricant.

In the analysis of the slip and twinning systems present, the laboratory coordinate system is chosen so that its axes are in the direction of cold rolling (DR), the normal to its plane (ND), and the transverse direction (TD), which is also the roller axis. Thus, the three directions form a right triad of vectors.

### INFLUENCE OF FRICTION

In the sample rolled without lubrication, deformation is due solely to slip, with the formation of deformation bands. As is well known, the rolling of single crystals with initial ribbed orientation (110)[001] leads to the formation of two symmetric orientations  $\{111\}\langle 112 \rangle$  in the form of sets of deformation bands separated by transition bands [17]. The experiment

allows us to trace the successive stages of this process (Figs. 1–3).

Even with relatively small deformation ( $\sim 18\%$ ), two deformation bands separated by a boundary are observed in a single crystal rolled with elevated friction (Fig. 1a). With greater deformation, the contact point of the deformation bands is characterized by microrelief at the surface of the section in the form of a network of slipping tracks (Luders lines), which intersect in the central region of the single crystal (Fig. 1b).

Orientalional analysis (EBSD) indicates the formation of deformation bands even with  $\sim 10\%$  deformation. Not two (as in Fig. 1a) but three deformation bands are formed at once in the single crystal studied; they differ somewhat in orientation. The boundary between them is not a strictly defined line but rather a region characterized by smooth transition from one orientation to the other. Orientalional analysis of the contact point of deformation bands reveals alternating microbands, each with slight different orientation, which are separated by small-angle boundaries. They become narrower toward the center of the single crystal (Fig. 2).

In the rolling of a (110)[001] single crystal with lubrication (reduced friction), twinning is observed even with small deformation (Figs. 1b and 3). Since twinning is always accompanied by the formation of the corresponding surface relief, it is natural to assume that the increased twinning in the alloy with lubrication is due to decrease in the contribution of surface energy to the total energy of twin nucleation.

With  $\sim 3\%$  deformation, twins of two symmetric systems (112)[ $\bar{1}\bar{1}1$ ] ( $T_1$ ) and (11 $\bar{2}$ )[ $\bar{1}\bar{1}\bar{1}$ ] ( $T_2$ ) are seen. Their orientations with respect to the laboratory coordinate system are (114)[ $\bar{2}\bar{2}1$ ] and (114)[ $22\bar{1}$ ], respectively (Fig. 3b). With  $\epsilon \geq 50\%$ , the twins of systems  $T_1$  and  $T_2$  are symmetrically aligned at angles 20°–25° and 155°–160°, respectively, with respect to the rolling plane (Figs. 3f and 3g). Then the twin density remains practically constant throughout the deformation pro-

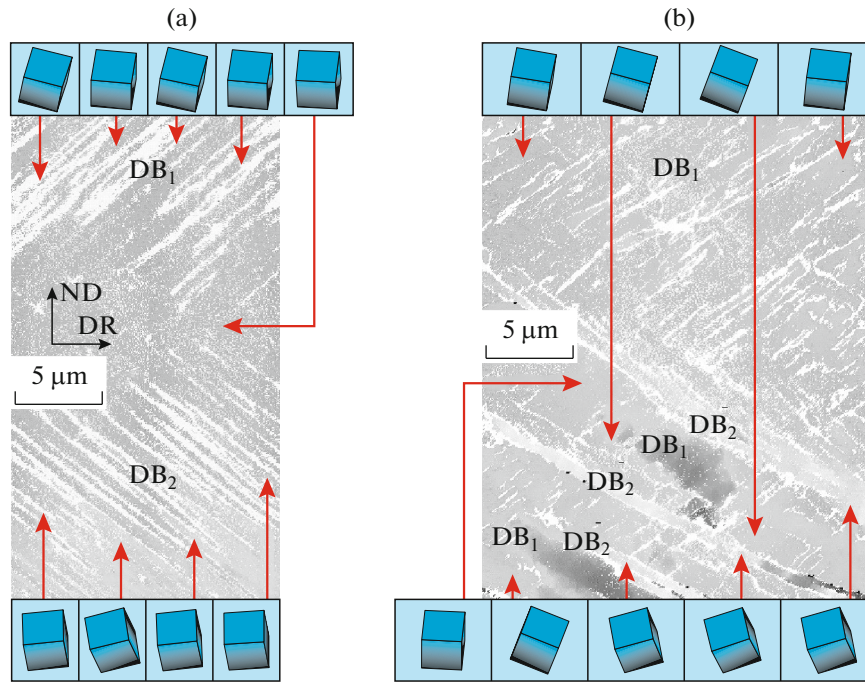


**Fig. 2.** Orientations of the central region of a single crystal rolled with elevated friction: orientation charts for the transverse direction. The orientations of individual local regions are shown as elementary cells of the crystal lattice. Deformation  $\epsilon \sim 18\%$  (a) and  $40\%$  (b). Notation: DB, deformation band.

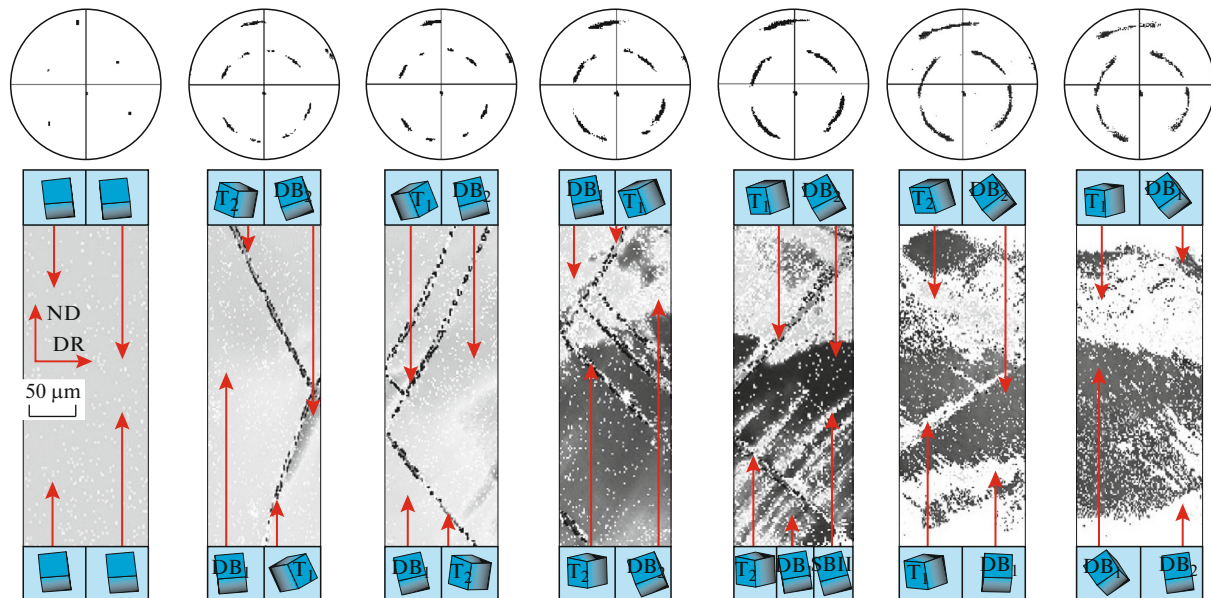


**Fig. 3.** Lattice reorientation of a single crystal rolled with reduced friction: orientation charts for the transverse direction (TD) and  $\{110\}$  pole figures with the corresponding charts. The orientations of individual local regions are shown as elementary lattice cells. Deformation  $\epsilon \sim 3\%$  (a),  $10\%$  (b),  $13\%$  (c),  $23\%$  (d),  $30\%$  (e),  $44\%$  (f), and  $54\%$  (g). Notation: SB, shear band.

cess. Orientational analysis shows that, throughout the whole deformation process, either the twins of both systems retain the strict  $\Sigma 3$  crystallographic relation with the matrix or else, on account of the local lattice reorientation,  $\Sigma 3$  disorientations are converted to similar special  $\Sigma 17b$  and  $\Sigma 43c$  disorientations.

In the rolling of single crystals with reduced friction, deformation is obviously due mainly to slip, which leads to the formation of deformation bands that differ in orientation (Fig. 3). Note that, in that case, one of the two visible deformation bands ( $DB_1$ ) basically retains the initial orientation of the single

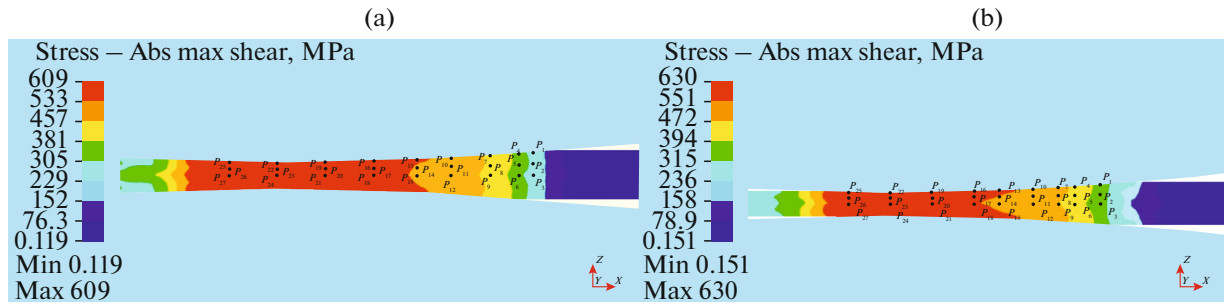


Fig. 4. Distribution of the stress  $\tau_{max}$  in the deformation zone when  $\mu = 0.11$  (a) and 0.22 (b) and positions of characteristic points.

crystal (Figs. 3a–3g). In the rolled single crystal with ~30% deformation, we may see traces of the spatial interaction of deformation bands in the form of bands ( $DB_2$ ) whose habitus plane is parallel to  $\{112\}$  (Fig. 3e).

Thus, rolling with and without lubrication (with different values of the frictional coefficient) will correspond to different deformation mechanisms, resulting in visible differences in the mesostructure and texture of the samples.

### CALCULATION RESULTS

We use Deform-3D software to analyze the influence of the frictional coefficient on the stress state in cold rolling. An elastoplastic model of the deformed

strip is chosen. Since the elastic deformation of the strip in cold rolling makes a small contribution to the total deformation, we adopt standard elastic properties for steel, without taking account of anisotropy: elastic modulus  $2.10 \times 10^5$  MPa; Poisson’s ratio 0.30. The plastic properties are described by means of the Mises condition; the resistance to deformation is determined from handbook data [18]. In rolling without lubrication, we assume a Coulomb frictional coefficient  $\mu = 0.22$ , as against  $\mu = 0.11$  with lubrication, in accordance with the recommendations of [19]. Then we consider the stress state in the center of the strip (over the width); rolling is assumed to be a steady process in modeling. In Deform-3D software, the stress  $\tau_{max}$  corresponds to the Abs. max shear function (Fig. 4).

Flow analysis is used for more detailed analysis of the distribution of stress  $\tau_{max}$  within the deformation zone. Since the deformation zone is symmetric, we consider only its upper half. The deformation zone is divided over the length into nine cross sections so as to cover all the regions of the stress diagram. In each section, we consider three characteristic points over the strip thickness: the surface ( $0.5h$ ), a quarter of the thickness ( $0.25h$ ), and the central layer (0). Thus, the stress  $\tau_{max}$  is estimated in nine cross sections over the length of the deformation zone, at three points over the thickness: 27 points in all (Fig. 4).

On the basis of Deform-3D software, we plot vector diagrams for the primary stress  $\sigma_1$  and  $\sigma_3$ . The direction of the tangential stress  $\tau_{max}$  may thus be determined as the bisectrix of the angle between the vectors  $\sigma_1$  and  $\sigma_3$ . In Fig. 5, we show the measured stress at the characteristic points and the angles between the rolling plane and the stress  $\tau_{max}$  at the characteristic points, for two different frictional coefficients.

For rolling with a large frictional coefficient, the tangential stress  $\tau_{max}$  for the corresponding cross sections of the deformation zone is greater overall than with a small frictional coefficient. This difference is more pronounced in the initial region of the deformation zone (Fig. 5). In addition, the difference in the frictional coefficient changes the direction of  $\tau_{max}$  over

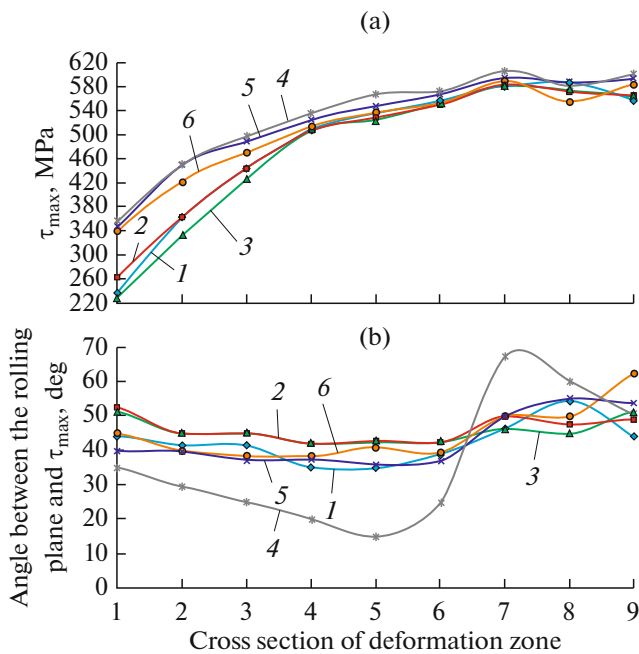


Fig. 5. Variation in the magnitude (a) and direction (b) of  $\tau_{max}$  over the length and depth of the deformation zone: (1, 4)  $0.5h$ ; (2, 5)  $0.25h$ ; (3, 6) 0;  $\mu = 0.11$  (1–3) and 0.22 (4–6).

the length and depth of the deformation zone, especially in the surface layers ( $0.5h$ ) of the strip. The considerable change in direction of  $\tau_{\max}$  in the surface layer of the deformation zone with increased frictional coefficient may be explained by the change in the direction of stress  $\tau_{\text{cont}}$  on passing from the kinematic lag zone to the lead zone.

Note that, for a low frictional coefficient in the initial region of the deformation zone, the angle between the rolling plane and the stress  $\tau_{\max}$  is close to  $55^\circ$ . This may explain the appearance of deformational twins in the structure with the given stress state (Fig. 1b), since the active twinning planes  $(112)$  and  $(11\bar{2})$  in the single crystal  $(110)\langle 001 \rangle$  are inclined at  $54.7^\circ$  to the rolling plane.

It follows from these results that the frictional coefficient may have significant influence on the stress state in the deformation zone. This qualitatively explains the experimental difference in structure of the single crystals rolled with different frictional coefficient.

### THE ROLE OF DISLOCATIONS

As soon as they are formed, all the deformation bands observed differ in lattice orientation from the initial orientation of the single crystal (Figs. 2 and 3). Even in the deformation band whose orientation is relatively close to the initial orientation, slip results in rotation of the lattice around both the rolling and normal directions. The reorientation of a lattice that deviates from the ideal orientation  $(110)[001]$  was analyzed in [15].

Overall, the reorientation of the  $(110)[001]$  single crystal may be described by lattice rotation in the deformation band around the crystallographic direction  $[1\bar{1}0]$ , which is close to the transverse direction. With increase in the deformation in rolling, we note further lattice reorientation in the basic volume of the deformation band, tending to two symmetric orientations  $\{111\}\langle 112 \rangle$  (Fig. 2b). Note that the formation of deformation bands occurs not only in the plane defined by the normal and rolling directions but also in the plane defined by the rolling and transverse directions: the relative volumes of the deformation bands in the same plane of the section may change significantly on motion in the rolling direction (Fig. 2). In Fig. 2b, the deformation band  $DB_2$  only exists as three narrow regions extending along the direction of slip of band  $DB_1$ . They may be regarded as mesostructural elements of shear-band type with the habitus plane  $\{112\}$  (SB II, according to [8]).

Obviously, the formation of deformation bands with a lattice tending to one of the two symmetric orientations  $\{111\}\langle 112 \rangle$  is associated with orientational instability of the initial crystal on rolling close to the crystallographic direction  $[001]$ . The appearance of a

set of deformation bands is due to local disorientation between sections of the initial single crystal. In different regions of its lattice, we note different primary slip systems, whose action determines the subsequent lattice reorientation. As a consequence, the deformation bands differ in the rate of lattice reorientation.

In the deformation of the  $(110)[001]$  single crystal in parallel planes  $\{112\}$ , series of dislocation loops extending along the shear direction  $\langle 111 \rangle$  are formed [1]. Loop formation within a single slip system  $\{112\}\langle 111 \rangle$  limits the path of the dislocations (the loop length) in the symmetric system (and vice versa). The choice of the slip system is random and determines the direction of lattice rotation toward one of the two orientations  $\{111\}\langle 112 \rangle$ . As a result, within the limits of a single deformation band, in the initial stages of its formation, microbands extending along the  $\langle 111 \rangle$  direction of the dominant (rotary) slip system are formed; these microbands are separated by small-angle boundaries, formed by segments of the edge dislocations of a second system. The disorientation between the microbands is no more than a few degrees, since dislocations of opposite sign approach the microbands from adjacent regions and practically cancel each other out, except for a small dislocation density of a particular sign. With increase in deformation and corresponding increase in the dislocation density, the disorientation between the microbands increases as the square root of the number of edge dislocations forming the given small-angle boundary. This is evidently the consequence of random fluctuation in the Burgers vector of the lattice dislocations along the crystallographic direction  $\langle 111 \rangle$ .

Along the slip direction of the dominant system, the microbands defined by small-angle boundaries are also divided by extended fragments. The corresponding transverse small-angle boundaries are formed by the edge components of the loops in the dominant system; disorientation of the fragments is again due to incomplete compensations of the signs of the dislocations.

Evidently, the fundamental difference between small-angle boundaries formed transverse to microbands and those in the direction of the microbands may be attributed to the higher mobility of the transverse microbands as the lattice takes on the corresponding orientation  $\{111\}\langle 112 \rangle$ . Under the action of the stress in the dominant slip system  $\{112\}\langle 111 \rangle$ , the transverse small-angle boundaries may break down as a result of the opposing motion of edge components of different sign. That increases the path length of the edge sections of the dislocation loop and correspondingly the degree of deformation in the given slip system. Thus, in the direction of slip, the fragments may combine, with increase in their length.

The formation of a transition band is fundamentally different from the formation of the small-angle boundaries separating microbands or arising within

microbands. Analysis of the active slip systems indicates that dislocations of a single sign, which repel one another, pass from the adjacent deformation bands (for example  $DB_1$  and  $DB_2$  in Fig. 2) to the transition band (at first, to the intermediate region). As a result, the structure of the intermediate region consists of a set of microbands with small-angle boundaries, which either continue to move or come to a halt. Obviously, with increase in the deformation, slip in the microbands from the transition region into the deformation band will be progressively blocked. The blocking is least along the effective slip system  $((110)[00\bar{1}](110)[\bar{1}\bar{1}\bar{1}] + (110)[1\bar{1}\bar{1}])$ . Thus, close to the deformation band (formed in the intermediate region), as a result of recoil of microbands from  $DB_1$  and  $DB_2$  and the associated blocking of slip in the dominant systems  $\{112\}\langle 111 \rangle$ , the orientation  $\{111\}\langle 112 \rangle$  becomes unstable and reverts to  $(110)[001]$  under the action of the effective slip system  $(110)[00\bar{1}]$ . When slip stops in the effective system on account of decrease in the Schmid factor, the inverse lattice rotation is made possible by the second active slip system  $\{112\}\langle 111 \rangle$ . As a result, the transition band may retain an orientation close to  $(110)[001]$  for a relatively long time during deformation.

An analogous mechanism explains the formation of the transition band inclined to the rolling plane that forms part of  $DB_2$ , with an orientation close to  $(110)[001]$  and a habitus parallel to the  $\{112\}$  plane of  $DB_1$  (Fig. 2b). Evidently, these bands are often wrongly interpreted as shear bands (SB II) [8, 12].

On the basis of the formation of crystalline structure in the deformation zone, we may also trace the sequence of twin reorientation in thinning of the band. In reorientation of the initial  $\{110\}\langle 001 \rangle$  single crystal to the direction  $\{111\}\langle 112 \rangle$ , the habitus of the twin system  $\{112\}\langle 111 \rangle$  aligned with the active slip system (for example, twin  $T_1$ ) should be inclined at  $\sim 20^\circ$  to the rolling plane. The orientation of the matrix with respect to the laboratory coordinate system will be close to  $(111)[\bar{1}\bar{1}2]$  ( $DB_1$ ), while that of twin  $T_2$  is  $(111)[\bar{1}\bar{1}2]$ . The habitus of twins of the second system  $T_2$  in  $DB_1$  should be practically perpendicular to the rolling plane, with a lattice orientation close to  $(111)[1\bar{1}\bar{2}]$ . Note, however, that decrease in the initial angle and retention of special disorientation is observed for both twin systems (Fig. 4). Their crystal lattice has the same orientation with respect to the matrix. In other words, one of the twin systems has the regular crystallographic position, while the other has an irregular position in the deformed matrix. The evolution of twin-system reorientation in the deformation zone with the retention of strict special disorientation of type  $\Sigma 3$  is fully described by the dislocation mechanisms in [20].

Thus, by EBSD, the structure formation in the cold rolling of a  $(110)[001]$  single crystal may be investigated directly within the deformation zone, as well as its relation to the stress state.

Obviously, the results here outlined do not fully account for the processes that occur in the deformation zone; further experimental and theoretical study is required. Nevertheless, it is clear that the stress state and frictional coefficient significantly affect the mesostructure formation and the development of crystalline texture. Research on functional materials with different submicro- and nanocrystalline structure is of great interest.

## CONCLUSIONS

We have investigated the mesostructure formation in cold rolling of  $(110)[001]$  single crystals of Fe–3% Si alloy within the deformation zone. Deform-3D software is used to calculate the stress state in rolling, for various values of the frictional coefficient. Depending on the frictional coefficient, the stress state may significantly affect the mesostructure formation and the texture development in the crystal.

On the basis of experimental data, we have proposed a dislocation model for the formation of deformational mesostructured in the cold rolling of a  $(110)[001]$  single crystal. This model includes the following components:

- the formation of microbands in the initial stage of deformation-band generation;
- the formation of transition bands parallel to the rolling plane with the dynamic retention of the initial orientation;
- the formation of transition bands inclined to the rolling plane with a habitus parallel to the  $\{112\}$  matrix plane.

We have traced the sequence of lattice reorientation of the twins when their special disorientation  $\Sigma 3$  with respect to the deformation matrix is retained.

## ACKNOWLEDGMENTS

This research was conducted in equipment in the laboratory of structural analysis and nanomaterials of the Center for Cooperative Use at Ural Federal University.

Financial support was provided by the Russian Foundation for Basic Research (project no. 17-08-00892).

We also appreciate support within the framework of Russian government decree no. 211 regarding the improved competitiveness of Russian universities (contract no. 02.A03.21.0006).

## REFERENCES

1. Vishnyakov, Ya.D. and Babareko, A.A., *Teoriya obrazovaniya tekstur v metallakh i splavakh* (Theory of Texture Formation in Metals and Alloys), Moscow: Nauka, 1979.
2. Humphreys, F.J. and Hatherly, M., *Recrystallization and Related Annealing Phenomena*, Amsterdam: Elsevier, 2004.
3. Furubayashi, E., Behavior of dislocation in Fe–3% Si under stress, *J. Phys. Soc. Jpn.*, 1969, vol. 27, no. 1, pp. 130–146.
4. Goncharov, V.A. and Karpov, M.I., Plastic deformation of (00-1) [–110] and (110) [–110] molybdenum single crystals by rolling at 293 K. Part 1. Crystallography of sliding, *Fiz. Met. Metalloved.*, 1976, vol. 42, no. 6, pp. 1305–1310.
5. Goncharov, V.A., Karpov, M.I., and Kopetskii, Ch.V., Plastic deformation of (00-1) [–110] and (110) [–110] molybdenum single crystals by rolling at 293 K. Part 2. Dislocation structure, *Fiz. Met. Metalloved.*, 1977, vol. 43, no. 6, pp. 173–179.
6. Perlovich, Yu.A., Isaenkova, M.G., and Fesenko, V.A., Regularities of substructural inhomogeneity of deformed metals, *Bull. Russ. Acad. Sci.: Phys.*, 2004, vol. 68, no. 10, pp. 1636–1646.
7. Lobanov, M.L., Danilov, S.V., Pastukhov, V.I., Averin, S.A., Khrunyk, Y.Y., and Popov, A.A., The crystallographic relationship of molybdenum textures after hot rolling and recrystallization, *Mater. Des.*, 2016, vol. 109, pp. 251–255.
8. Ushioda, K. and Hutchinson, W.B., Role of shear bands in annealing texture formation in 3% Si–Fe (111)[11 $\bar{2}$ ] single crystals, *ISIJ Int.*, 1989, vol. 29, pp. 862–867.
9. Hutchinson, B., Deformation substructures and recrystallization, *Mater. Sci. Forum*, 2007, vols. 558–559, pp. 13–22.
10. Dorner, D., Zaefferer, S., and Raabe, D., Retention of the Goss orientation between microbands during cold rolling of an Fe–3%Si single crystal, *Acta Mater.*, 2007, vol. 55, no. 7, pp. 2519–2530.
11. Dorner, D., Adachi, Y., Tsuzaki, K., and Zaefferer, S., Tracing the Goss orientation during deformation and annealing of an FeSi single crystal, *Mater. Sci. Forum*, 2007, vol. 550, pp. 485–490.
12. Rusakov, G.M., Lobanov, M.L., Redikul'tsev, A.A., Karabanalov, M.S., and Lobanova, L.V., Special misorientations in localized deformation regions in Fe–3% Si alloy single crystals, *Tech. Phys.*, 2014, vol. 59, no. 8, pp. 1180–1184.
13. Xiuhua, G., Kemin, Q., and Chunlin, Q., Magnetic properties of grain oriented ultra-thin silicon steel sheets processed by conventional rolling and cross shear rolling, *Mater. Sci. Eng. A*, 2006, vol. 430, no. 1, pp. 138–141.
14. Heo, N.H., Soh, J.Y., Oh, J.M., and Kim, S.B., Influence of cold-rolling texture and heating rate on {110}<001> development in inhibitor-free 3%Si–Fe sheets, *J. Magn. Magn. Mater.*, 2008, vol. 320, no. 20, pp. 635–637.
15. Lobanov, M.L., Redikul'tsev, A.A., Rusakov, G.M., Kagan, I.V., and Pervushina, O.V., Effect of the grain orientation in the material used for the preparation of an ultrathin electrical steel on its texture and magnetic properties, *Phys. Met. Metallogr.*, 2011, vol. 111, no. 5, pp. 479–486.
16. Lobanov, M.L., Rusakov, G.M., and Redikul'tsev, A.A., Effect of copper content, initial structure, and scheme of treatment on magnetic properties of ultra-thin grain oriented electrical steel, *Phys. Met. Metallogr.*, 2013, vol. 114, no. 7, pp. 559–565.
17. Sokolov, B.K., Sbitnev, A.K., Gubernatorov, V.V., Gervasyeva, I.V., and Vladimirov, L.R., On the influence of the annealing heating rate on the recrystallization texture of a deformed single crystal (110) [001] of 3% silicon iron, *Textures Microstruct.*, 1995, vols. 26–27, pp. 427–443.
18. Tret'yakov, A.V. and Zyuzin, V.I., *Mekhanicheskie svoistva metallov i splavov pri obrabotke davleniem* (Mechanical Properties of Metals and Alloys under Pressure), Moscow: Metallurgiya, 1973.
19. Grudev, A.P., *Vneshnee trenie pri prokatke* (External Friction at Rolling), Moscow: Metallurgiya, 1973.
20. Rusakov, G.M., Lobanov, M.L., Redikul'tsev, A.A., and Kagan, I.V., Retention of the twinning  $\Sigma 3$  misorientation in the process of lattice transformation during cold rolling of a Fe<sub>3</sub>Pct Si single crystal, *Mater. Trans. A*, 2011, vol. 42, no. 6, pp. 1435–1438.

*Translated by Bernard Gilbert*